

# Representing subgrid scale mixing under stable conditions: Importance for overall model synoptic development.

Colin G. Jones<sup>1</sup>, Geert Lenderink<sup>2</sup> & Karl-Ivar Ivarsson<sup>1</sup>

<sup>1</sup>SMHI

<sup>2</sup>KNMI

## 1. Introduction and Motivation

In 2002 SMHI began testing a new operational forecast version of the HIRLAM model. Hereafter this new model will be referred to as HIRLAM-X. A number of parameterisation schemes were newly introduced in HIRLAM-X, among these the subgrid scale vertical diffusion scheme was changed from the K-diffusion Louis scheme (Louis 1979) to the turbulent kinetic energy (TKE) based CBR scheme (Cuxart et al. 2000, Lenderink 2003). On making this change TKE became a prognostic variable in the model system. In evaluating the new model system four separate months were simulated, one from each season, with the original operational model and with the HIRLAM-X model. Comparison of the forecasts from these periods, against observations, indicated that low pressure systems traversing Europe and Scandinavia were systematically too deep in the HIRLAM-X model (ie. the model exhibited a negative Mean Sea Level Pressure (MSLP) bias preferentially around regions of low pressure systems). Associated with these biases the Root-Mean-Squared (RMS) error of MSLP, when evaluated against EWGLAM stations grew at an unacceptably large rate through the forecast period.

After extensive analysis of typical synoptic simulation failures, it became apparent that the overall synoptic scale evolution of the model atmosphere was very sensitive to the representation of subgrid scale vertical mixing in statically stable conditions (*in particular the mixing of momentum*). Due to a strong inter-relationship between model static stability, prognostic TKE, diagnosed mixing lengths in stable conditions and subgrid scale vertical fluxes the model atmosphere is very sensitive to the calculation of the diagnostic mixing length used for determining vertical turbulent fluxes in stable situations. Increasing this mixing length and thus the turbulent flux of momentum in the mid to lower troposphere in stable grid columns, led to a systematic filling of low pressure systems compared to the original HIRLAM-X model and a large reduction in the RMS and bias values of MSLP and geopotential throughout the model atmosphere. It was also noted that anticyclonic situations became less anticyclonic (weaker high pressures) when increased momentum mixing in stable conditions was introduced. This change also improved the original positive HIRLAM-X bias (*i.e. too high surface pressures*) in MSLP during anticyclonic situations. The wind speeds through the depth of the model atmosphere were decelerated from a general positive bias of 0.2-1ms<sup>-1</sup> closer to a zero bias. This occurred through increased downward mixing of momentum by turbulence and is the primary cause of the associated large scale synoptic circulation improvements. Four separate weeks (one from each season of the original HIRLAM-X comparison forecasts) were repeated with the HIRLAM-X model including two modifications that increased turbulent mixing in statically stable conditions. Figure 1 & 2 compare the integrated results (bias & RMS) of the near surface and free troposphere variables from the original HIRLAM-X model and the new version with increased mixing. Results are presented from a comparison against all available EWGLAM stations. MSLP and

geopotential RMS and bias are improved in all seasons, as is the free tropospheric wind speed bias. The one degradation is an increase in an existing positive bias in the 10m wind speed. This feature requires further investigation. Precipitation scores were also seen to improve relative to the original HIRLAM-X forecasts for the weeks tested (results not shown). This relative improvement increased with forecast length and we believe results from a better overall evolution and therefore placement in space and time of the rain bearing synoptic systems in the new model.

In this note we motivate from physical arguments the modifications to the mixing calculation in stable conditions, describe these modifications and briefly explain the physical processes occurring in synoptic systems that leads to the overall forecast improvements.

## **2. Balanced response of the model dynamics to increased subgrid scale mixing.**

As seen in figure 2, over a large depth of the model atmosphere wind speeds were reduced (towards zero bias) in the new model, this occurs as a result of increased subgrid scale downward momentum mixing (*in stable conditions*) in the new HIRLAM-X model. Divergence of the vertical turbulent momentum flux leads to a local deceleration of the wind velocities. Following geostrophic theory, the locally reduced wind speeds will be accompanied by a reduced pressure gradient (i.e. in low pressure situations a reduction in the pressure gradient between the cyclone centre and the surrounding model atmosphere). In essence the mass field will adjust to the velocity field to retain (quasi) geostrophic balance. The local reduction in momentum, induced by downward momentum mixing, will cause an ageostrophic flow component directed down the pressure gradient towards the low pressure centre. This ageostrophic flow will occur at all levels experiencing a local layer reduction in momentum due to turbulent mixing. A net mass transfer into the low pressure centre will occur at these levels due to this ageostrophic convergence. The mass transfer will lead to a local reduction in the geopotential and pressure gradients associated with a low pressure system and an overall increase in the central pressure of the cyclonic system. In the model version with increased momentum mixing in stable conditions, the downward mixing of momentum will be more vigorous in stable regions. Around cyclone centres, the HIRLAM model exhibits large regions of stability throughout the depth of the model atmosphere. In these regions, downward momentum flux due to parameterised turbulence will be stronger in the new model and the ageostrophic mass convergence, to the low pressure side of the regions of enhanced momentum mixing, will be increased. This will result in increased mass convergence into the low pressure centres in the new model version. As a direct consequence of this, the surface pressure around the cyclone centre (inward from the region of increased momentum mixing) will increase and an overall reduction in the pressure and geopotential gradients in the new model version will ensue.

A similar physical process occurs in anticyclonic situations and leads to turbulent momentum mixing *reducing* the central pressure of anticyclones and again weakening the overall pressure gradient in these systems. Downward mixing of momentum will again induce an ageostrophic flow directed down the pressure gradient. In this case ageostrophic mass divergence out of the anticyclonic (high pressure) centre will occur and a reduction in mass and surface pressure around the anticyclone centre will be seen. In the anticyclonic case, a relative increase in mass divergence and decrease in pressure will occur to the high pressure side of the region of increased downward turbulent momentum flux in the new HIRLAM-X model (i.e. at and

around the central region of high pressure systems, where stable situations are extremely common).

### 3. The relationship between prognostic TKE, subgrid scale mixing and stability in the HIRLAM model

Here we detail the subtle links that exist between the HIRLAM model TKE field, static stability and turbulent fluxes and motivate some modifications to the turbulence scheme that ultimately lead directly to an increase in turbulent mixing (primarily of momentum). Following previous HIRLAM reports we will refer to the TKE based turbulent scheme used in the HIRLAM-X model as CBRGL. The original formulation is detailed in Cuxart et al. (2000) and a new approach to calculating the mixing lengths controlling the vertical fluxes is described in Lenderink (2003). Here we briefly review the important aspects of the CBRGL turbulence scheme and illustrate the tight coupling that exists between vertical stability, TKE evolution and subgrid scale vertical fluxes.

The time rate of change of a variable  $\chi$  due to subgrid scale turbulence results from the vertical convergence of the subgrid scale fluxes. Where the parameterised subgrid fluxes are represented by:

$$\overline{\omega' \chi'} = K_{\chi} \frac{\partial \overline{\chi}}{\partial z} \quad 1$$

Where  $\chi$  is any of the model prognostic variables and  $K_{\chi}$  is the eddy diffusivity of the grid box mean value. An overbar denotes a grid box mean value and primes denote deviations from the mean values. In the CBRGL TKE based mixing scheme, the eddy diffusivity depends on a diagnosed mixing length, considered representative of the subgrid scale eddies performing the majority of the mixing and the grid box mean TKE value.

$$K_{\chi} = l_{\chi} \overline{e}^{1/2} \quad 2$$

The vertical turbulent fluxes of all prognostic variables therefore depend directly on the evolution of the TKE field (denoted  $e$  in all equations). The evolution of TKE follows the prognostic TKE equation, which can be expressed in 2 dimensions as:

$$\frac{\partial \overline{e}}{\partial t} + \overline{u} \frac{\partial \overline{e}}{\partial x} = \frac{g}{\theta_v} (\overline{\omega' \theta'_v}) - \overline{u' \omega'} \frac{\partial \overline{u}}{\partial z} - \frac{\partial}{\partial z} \left( \overline{\omega' e'} + \frac{\omega' p'}{\rho} \right) - C_d \frac{\overline{e}^{3/2}}{l_{\epsilon}} \quad 3$$

The first term on the right hand side (rhs) represents the production or destruction of TKE due to buoyancy forces, the second term is production of TKE due to vertical shear of the horizontal wind field. The third term in parentheses is the transport of TKE due to vertical diffusion and pressure covariance. The last term represents the dissipation of TKE, where  $C_d$  is a constant and  $l_{\epsilon}$  is a dissipation length scale (*In the CBRGL scheme the dissipation length scale and momentum length scales are presently set equal.*) From equations 1 and 2, the first terms on the rhs of the TKE equation are functions of a diagnostic mixing length and the

prognostic TKE. In this manner, the evolving TKE values control the vertical fluxes of heat and momentum, which in turn through equation 3, control the evolution of the TKE field. i.e.

$$\overline{\omega' \theta_v'} = l_h e^{1/2} \frac{\partial \overline{\theta_v}}{\partial z} \quad 4$$

In the following section we will describe the calculation of the mixing lengths for heat ( $l_h$ ), momentum ( $l_m$ ) and dissipation ( $l_\epsilon$ ) in the CBRGL scheme under statically stable conditions. We will suggest that these mixing lengths are too rapidly reduced as stability increases. Considering equations 2, 3 & 4 one can see that there is a strong feedback loop between TKE, stability and vertical fluxes. If the mixing lengths are underestimated (for whatever reason) then the vertical fluxes will also be underestimated and the TKE production terms (first and second on rhs of equation 3) will be erroneously small. The small mixing lengths will also lead to large dissipation rates through the last term in equation 3. The net result will be that prognostic TKE values will be rapidly reduced in stable regions. The small TKE values will directly lead to even smaller vertical turbulent fluxes, through the presence of TKE in equation 4. The underestimated turbulent fluxes will also lead to enhanced stability and a further reduction in the diagnosed mixing lengths, these being inversely proportional to stability and as a consequence a further reduction of TKE will ensue. Any tendency for a model to either predict excessive stability or underestimate mixing lengths in stable situations will therefore allow this feedback loop to activate and increase stability and reduce mixing still further.

In CBRGL the mixing length that appears in equation 2, is a combination of a diagnosed (neutral/unstable) mixing length resulting from integration over measures of column stability (ie the Richardson Number) and a separate stable mixing length. Also, close to the ground the diagnosed mixing length is forced to converge towards values conforming to Monin-Obhukov surface similarity theory (e.g. see Businger 1971). Details of the overall strategy for determining the mixing length can be found in Lenderink (2003). In stable situations above the lowest model layer, the diagnosed stable mixing length largely determines the resulting mixing length used to define the eddy diffusivity and control the resulting vertical turbulent fluxes. We therefore concentrate on this mixing length here, it is modifications to this calculation that we have introduced into the HIRLAM-X model leading to the results in Figures 1 & 2.

At regions of grid column stability the CBRGL scheme uses a mixing length formulation following the original suggestion of Deardorff (1974).

$$l_s = C_{(m,h)} \frac{e^{1/2}}{N} \quad \text{where} \quad N^2 = g \frac{\partial \overline{\theta_v}}{\partial z} \quad 5$$

$l_s$  is the diagnosed stable mixing length,  $C_{(m,h)}$  is a constant (*the subscript m,h indicating values applied for momentum and heat/water mixing lengths respectively. These constants being equal in the original CBRGL scheme.*)  $N^2$  is the Brunt-Väisälä frequency, a measure of the *grid box mean* stability diagnosed as a gradient between adjacent full level virtual potential temperatures ( $\theta_v$ ). Following the earlier arguments one can see that there is potential, through an initial underestimate of stable mixing lengths (via equation 5), for an underestimate of the vertical fluxes (equation 4) and a subsequent decrease in TKE values

through small production and large dissipation terms in the TKE prognostic equation 3. Small vertical fluxes will further increase in the grid box mean stability. Both of the latter two effects will (all other things being equal) contribute to an even smaller  $l_s$  next timestep (i.e. smaller values of TKE and larger values of N). This feedback loop makes the diagnosis of the stable mixing length an extremely important component of the model turbulence scheme. Furthermore, the model (*and real*) atmosphere naturally prefers to reside in a stable state, leading to the turbulent fluxes often being dominated by fluxes in stable situations. One can rewrite the TKE prognostic equation to further highlight the central role TKE and stability play in the overall evolution of the model prognostic TKE field and by implication the subgrid scale vertical fluxes. Substituting equations 4 and 5 into 3 one gets for stable conditions:

$$\frac{\partial \bar{e}}{\partial t} + \bar{u} \frac{\partial \bar{e}}{\partial x} = \frac{g^{1/2}}{\bar{\theta}_v} \left( C_h e \left( \frac{\partial \bar{\theta}_v}{\partial z} \right)^{1/2} \right) - \frac{C_m e}{g^{1/2} \left( \frac{\partial \bar{\theta}_v}{\partial z} \right)^{1/2}} \left( \frac{\partial \bar{u}}{\partial z} \right)^2 - \frac{C_d C_m e^2}{g^{1/2} \left( \frac{\partial \bar{\theta}_v}{\partial z} \right)^{1/2}} \quad 6$$

The evolution of TKE is seen to be strongly a function of TKE itself and the vertical shear of the grid box mean virtual potential temperature (stability) and mean wind field.

Equation 5, for the stable mixing length was originally proposed by Deardorff (1974) for representing stable mixing in a large eddy simulation model (LES), using grid dimensions of the order 50 metres. It is questionable whether this equation is directly applicable to an NWP model with a grid resolution of typically 10-50km in the horizontal and 100-1000 metres in the vertical. In particular, the degree of (organised) subgrid scale variability (in both the horizontal and vertical) contributing to unresolved vertical transports may be greater for grid resolutions used in NWP models compared to LES models. As an example, thin vertical jets are known to frequently develop in Stable Boundary Layers (SBLs) (Mahrt 1999) The vertical shear in the wind field around these jets, will directly contribute to a vertical momentum flux and the maintenance of turbulence in SBLs. Due to the low vertical resolution of NWP models, these jets will frequently not be resolved (*even if the physics generating them is present in the models*). Ideally, the effect of these *unresolved* jets on the *parameterised subgrid scale* vertical transport of momentum should be included.

There are strong observational and theoretical arguments suggesting that the form of stable mixing length given by equation 4 underestimates vertical mixing, particularly with respect to momentum in high stability regimes. Kosović & Curry (2000) recently performed very high resolution (~10m grid box sizes in all 3 dimensions) LES simulations of a variety of SBLs. (*For very high stability regimes, very high resolution is needed to explicitly simulate the eddies performing the turbulent mixing. These resolutions have only recently become attainable through increased computer power.*) Their results indicate that the vertical fluxes of heat and momentum remain a significant fraction of the flux values at neutral conditions. At a Richardson number of  $1/2$ , their LES results show vertical momentum fluxes ~25% of

neutral values and heat fluxes ~10% of neutral values (*see their figures 3 & 4*), with the respective fluxes asymptoting to this flux magnitude and not towards zero, as is commonly assumed for Richardson numbers beyond some assumed critical value (often of order ~0.2). Cheng et al (2002) recently developed a new parameterisation of subgrid scale mixing within the original Mellor & Yamada (1974) framework. The results of their scheme agree well with the findings of Kosovic & Curry (see Figures 9 & 10 in Cheng et al.), with momentum and heat mixing remaining a significant fraction of their respective values at neutral conditions even at Richardson Numbers of 0.5. Furthermore, Cheng et al found that the ratio of the eddy diffusivities of momentum and heat (normalised by their respective values at neutral conditions) increased from unity to ~5 as the Richardson number increased from 0 to 1. This finding is supported by the observations of Kim & Mahrt (1992). Using aircraft observations they determined that the ratio of the eddy diffusivities of momentum and heat are a near linearly increasing function of Richardson Number in the observed Ri No spectrum. One mechanism assumed responsible for maintaining (at least momentum) mixing in high stability regimes is the presence of internal gravity waves in stably stratified fluids allowing an *upscale* cascade of energy extracted by eddies in the form of dissipation (Canuto & Minotti 1993). In order to include the above findings in our parameterisation of subgrid scale momentum flux, we allow the constant  $C_m$  (used for calculating momentum mixing lengths in stable situations in equation 5) to vary as a linear function of increasing Richardson Number.

$$C_m = pff(p) \cdot [C_h \cdot \max((1 + 3Ri), 10)] \quad 7$$

where the Richardson Number is calculated as follows using grid box mean values:

$$Ri = \frac{\frac{g}{\theta_v} \frac{\partial \overline{\theta_v}}{\partial z}}{\left| \left( \frac{\partial \overline{U}_{i,j}}{\partial z} \right)^2 \right|} \quad 8$$

$C_h$  equals 0.2 and is the constant used for the heat mixing length in equation 5,  $pff(p)$  varies linearly from a value of unity at the surface to zero at and above 100hpa. This crudely mimics our belief that the majority of internal gravity waves, inducing turbulent mixing, occur near the surface and in shallow near surface SBLs. This term was also necessary to avoid (*apparent*) excessive turbulent mixing close to the tropopause.

Mahrt (1987) has also discussed extensively the impact of subgrid scale variability of vertical stability on area-averaged vertical fluxes. For an area of ~30km x 30km (i.e. the scale of a typical model grid box) the area-averaged vertical gradient of virtual potential temperature may indicate mean stable conditions. But the vertical flux of some variable (e.g. heat or momentum) calculated from the area-mean stability, may often be significantly smaller than the area-averaged vertical flux calculated from the individual “subgrid scale” entities of the 30km<sup>2</sup> box. i.e.

$$K_{m,h} \left( \frac{\partial \overline{\theta_v}}{\partial z} \right) < K_{m,h} \left( \frac{\partial \sum_{i=1}^N \theta_{vi}}{\partial z} \right) \quad \text{even though} \quad \overline{\frac{\partial \theta_v}{\partial z}} = \sum_{i=1}^N \frac{\partial \theta_{vi}}{\partial z} \quad 9$$

As put by Mahrt (1987), “*The exchange coefficient predicted by the area-averaged stability may be quite small in stable conditions. However due to the strong nonlinearity of the stability dependence, the area-average of the local exchange coefficient may be significantly larger due to subgrid areas where the stratification is near-neutral or unstable*”. In these local regions of reduced stability the fluxes will be an order of magnitude larger than the grid box mean calculated values and therefore will contribute a disproportionately large fraction to the grid box mean vertical flux. Ideally, one would like to link this type of flux enhancement in stable conditions to some measure of the subgrid scale variability generating subregions of flux enhancement. This is a difficult problem though. Here we follow Mahrt (1987) and based on aircraft observations he presented, showing that the standard deviation of Richardson Number increases as the observed spatially meaned Richardson Number increases, we parameterise the flux enhancement due to subgrid scale regions of reduced stability by linking it to the Richardson Number. This is similar to suggested by Mahrt (1987) and originally followed in the Louis mixing scheme (Louis 1979). In grid columns that are stable with respect to the grid box mean virtual potential temperature, we calculate the stable mixing length ( $l_m$  &  $l_h$ ) through equation 5, using the modified  $C_m$  constant from equation 7 that represents enhanced momentum mixing due to internal gravity waves, or  $C_h$  equal to 0.2 for heat and water. We then further modify the two stable mixing lengths by applying the following formula below a diagnosed boundary layer top.

$$l'_{m,h} = l_{m,h} \times \left( \min \left( \exp \left( 0.5 Ri^{0.2} \right), 2.5 \right) \right) \quad 10$$

This form makes the  $l'_{m,h}$  value increase relative to  $l_{m,h}$  as a weak function of the Richardson Number. The modified mixing length is that which finally goes into equation 2 for calculating the vertical turbulent fluxes and into equation 3 for prognostication of the TKE field. The mixing length for dissipation ( $l_e$ ) is finally set equal to the modified momentum mixing length and used in equation 3. This set of modifications, apply to all calculations of free atmospheric turbulent mixing that use the diagnosed mixing lengths. They have also been introduced into the new moist conservative version of the CBRGL scheme, see Tijm (2003) this newsletter. As noted there and seen in other simulations, as well as impacting on the model synoptic scale the changed mixing in stable conditions has a profound impact on the evolution of the model boundary layer structure. In particular, increased mixing at the top of the boundary layer increases entrainment into the boundary layer and the overall growth rate of the boundary layer is increased. The net result is a deeper boundary layer that is drier and warmer. Clouds forming at the top of the well mixed boundary layer will also lie at a slightly high level.

Presently, the surface fluxes in HIRLAM still follow the updated Louis formulation in stable situations (Louis et al. 1981). The increased downward mixing of momentum through the model atmosphere, associated with the changes reported here, lead to an acceleration of the lowest model level wind speed. As seen in Figure 1 this leads to an increase in a pre-existing positive bias in the 10m wind field. The representation of the surface flux of momentum (and possibly heat) may need revisiting to make them more consistent with the modified

atmospheric turbulence and improve the lowest level wind field. Apart from this deviation, we believe these modifications greatly improve the overall dynamical, synoptic scale evolution of the HIRLAM model forecasts.

## References

- Businger, J.A., J.C.Wyngaard, Y Izumi and E.F.Bradley 1971: Flux profile relationships in the atmospheric surface layer. *J. Atmos. Sci* **28**, 181-189
- Cheng Y., V.M.Canuto and A.M.Howard 2002: An Improved Model for the Turbulent PBL. *J.Atmos Sci* **59**, 1550-1565
- Cuxart J., Ph Bougeault and J-L Redelsperger 2000: A turbulence scheme allowing for meoscale and large-eddy simulations. *Quart. J. Roy. Met. Soc* **126**, 1-30
- Deardorff J.W. 1974: Three dimensional numerical study of the height and mean structure of a heated planetary boundary layer. *Bound. Layer Meteor.* **7**, 19-226
- Louis J-F, Tiedtke M and J-F Geleyn 1981: A short history of the operational PBL parameterisation at ECMWF. *Workshop on the Planetary Boundary Layer Parameterisation. ECMWF Workshop Proceedings. 25-27 November 1981.*
- Kim J., L.Mahrt 1992: Simple formulation of turbulent mixing in the stable free atmosphere and nocturnal boundary layer. *Tellus* **44A**, 381-394
- Kosović B., and J.A. Curry 2000: A Large Eddy Simulation Study of a Quasi-Steady, Stably Stratified Atmospheric Boundary Layer. *J. Atmos. Sci* **57**, 1052-1068
- Lenderink G. 2003: An Integral Mixing Length Formulation for a TKE-1 Turbulence Closure in Atmospheric Models. *Submitted to Mon. Wea. Rev.*
- Louis J-F 1979: A parametric model of vertical fluxes in the atmosphere. *Bound. Layer Meteor* **17**, 187-202.
- Mahrt L 1987: Grid-Averaged Surface Fluxes. *Mon. Wea. Rev.* **115**, 1550-1560
- Mahrt L 1999: Stratified Atmospheric Boundary Layers. *Bound. Layer Meteor* **90**, 375-396
- Mellor G.L. and T.Yamada 1974: A hierarchy of turbulence closure models for the planetary boundary layer. *J. Atmos. Sci* **31**, 1791-1806
- Tijm A.B.C 2003: This edition of HIRLAM Newsletter

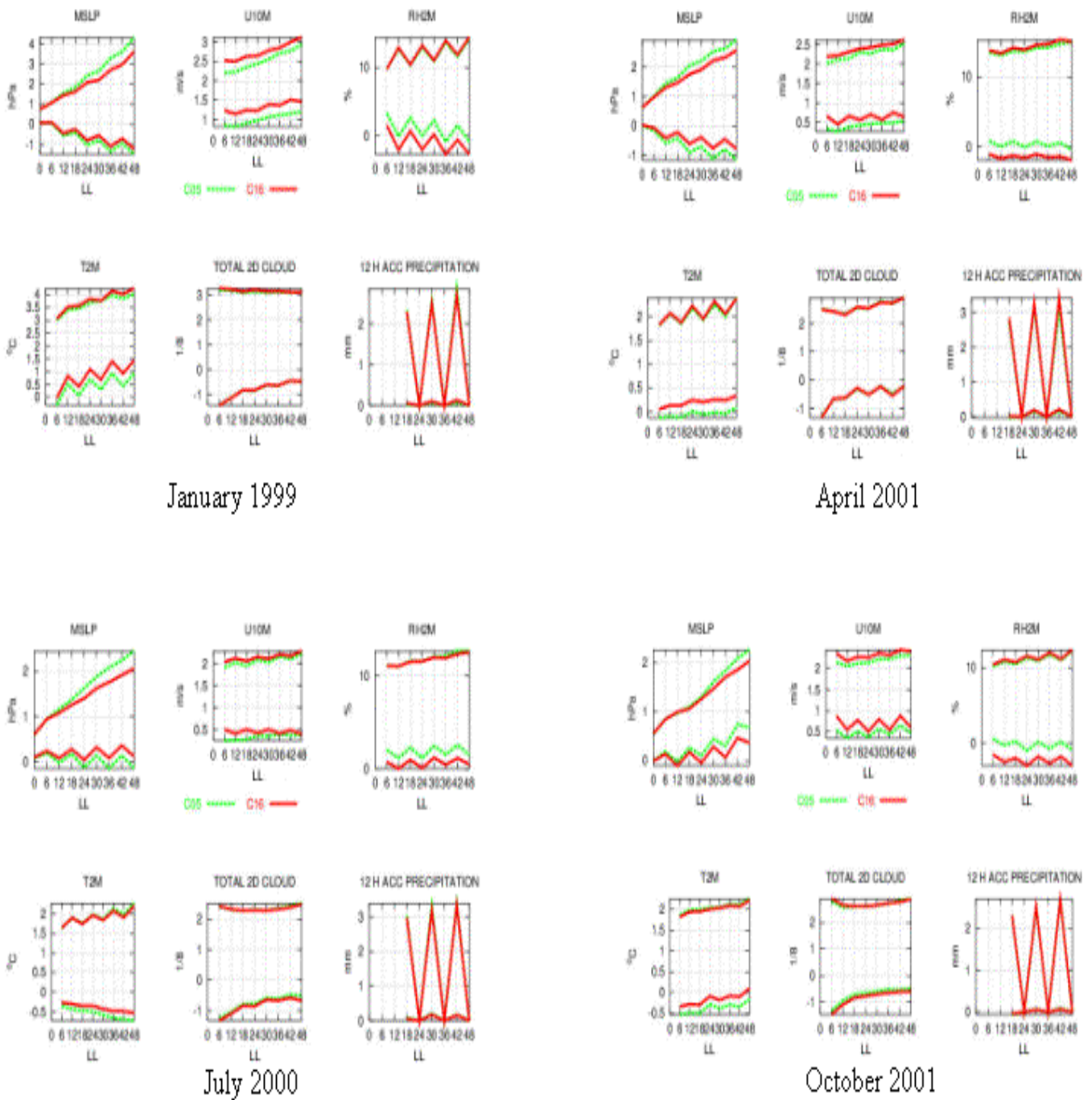
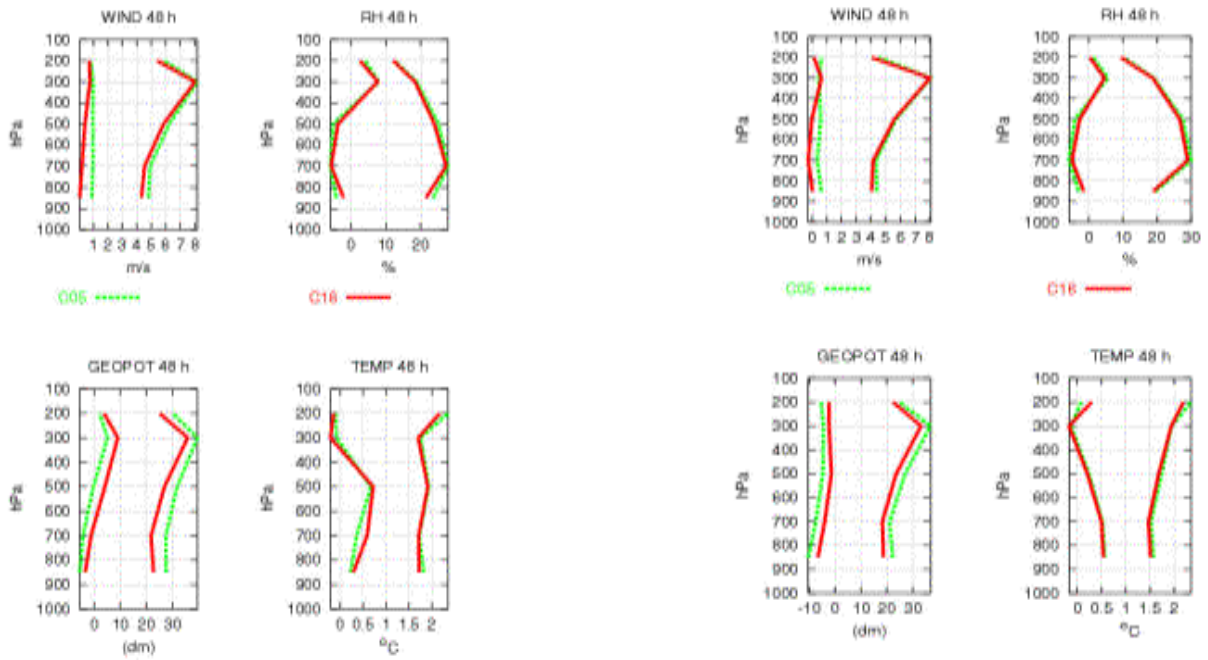
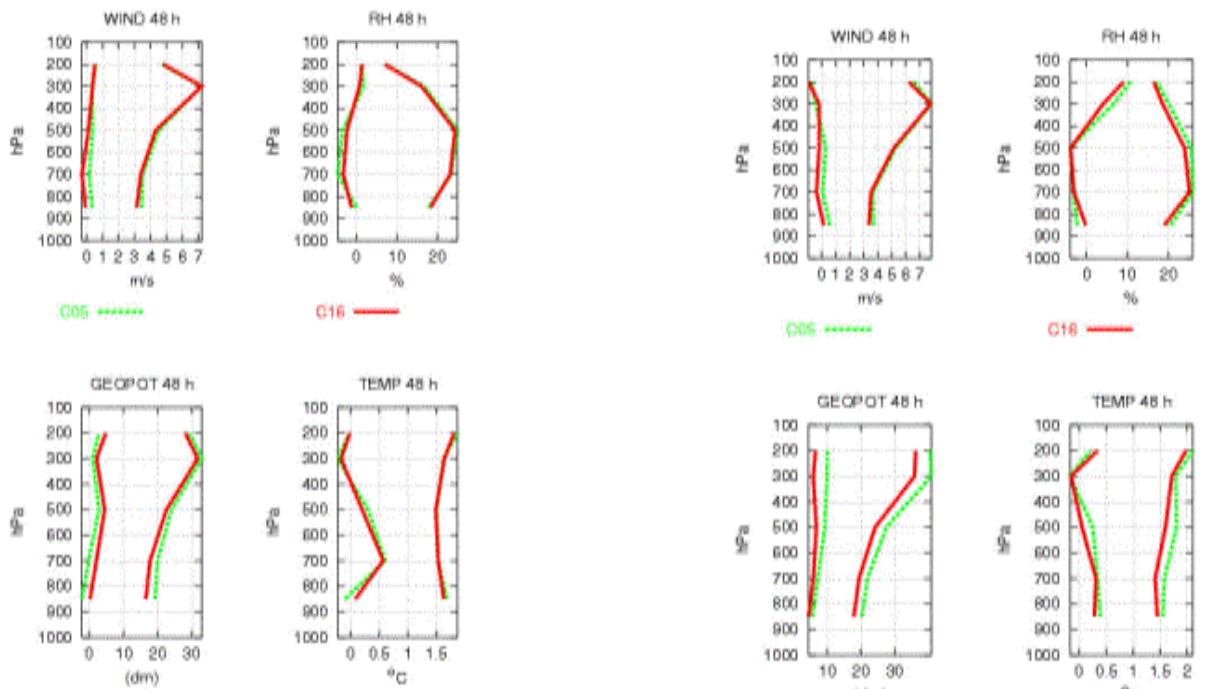


Figure 1. Model bias and Root Mean Square Error over the 48 hour forecast period for MSLP, 10m wind speed (U10M), 2 metre temperatures (T2M), 2 metre relative humidity (RH2M) and total cloud cover. *The precipitation results are not representative and should be ignored.* Green curve is for original HIRLAM-X model and red is for HIRLAM-X with modified mixing lengths in stable conditions.



January 1999

April 2001



July 2000

October 2001

Figure 2 Model bias and Root Mean Squared error of wind speed, relative humidity (RH), geopotential and temperature derived from comparison to all EWGLAM stations within the HIRLAM-X model domain. Comparison is made over the forecast period 12-48 hours for 4 forecasts per day for a week long period of each month highlighted. Green curve is the original HIRLAM-X model, red is HIRLAM-X with modified mixing lengths in stable conditions.